

Cite this: *Energy Environ. Sci.*,  
2026, 19, 2922

# Safeguarding drinking water in north-western Europe by modelling the fate of amines from CO<sub>2</sub> capture

François Clayer,<sup>id</sup>\*<sup>ab</sup> Cathrine Brecke Gundersen,<sup>a</sup> Magnus Norling,<sup>a</sup>  
Luca Pozzoli,<sup>c</sup> Ashenafi Seifu Gragne<sup>a</sup> and Tore Flatlandsmo Berglen<sup>c</sup>

The European Union (EU) net-zero emission target for 2050 requires large-scale deployment of carbon capture and storage (CCS). Amine-based CO<sub>2</sub> capture (CC) is the most mature CC technology but may lead to the spread of nitrosamines (NSAs) and nitramines (NAs) in the nearby surroundings. These are carcinogenic compounds that can persist in water resources. Hence, EU's ambition towards carbon neutrality might pose risk of drinking water contamination as well as ecosystem and agricultural crops pollution. We compiled a dataset of planned CCS projects in the Franco-Danish corridor, Europe's future CCS hub, where most capacity will be located by 2030, with at least 40% based on amine technology. Spatial analysis indicates that up to 10.2 million inhabitants, large Natura 2000 reserves, and extensive crop areas may be impacted by NA and NSA deposition, often in regions already under severe water stress. Biogeochemical modelling shows that surface waters with short residence times are highly sensitive to deposition rates, whereas groundwater concentrations depend strongly on the interplay between NA and NSA half-lives and travel times, creating greater uncertainty in aquifers, especially small systems with limited dilution. In both cases, MEA is the most environmentally friendly when emission abatement measures are limited to water wash, compared to piperazine and other emerging solvents. Main findings highlight the need for regional-scale modelling and harmonized regulation to safeguard drinking water, ecosystems, and food security as CCS deployment expands.

Received 2nd December 2025,  
Accepted 20th March 2026

DOI: 10.1039/d5ee07330h

rsc.li/ees

## Broader context

Carbon capture and storage (CCS) is essential for meeting the EU net-zero climate target by 2050, yet its large-scale deployment raises new environmental challenges. Amine-based capture, the most mature technology, can lead to the dispersion of nitrosamines and nitramines—carcinogenic compounds that may contaminate drinking water, ecosystems, and crops. The problem addressed is how to quantify the spatial extent and cumulative burden of these emissions in regions where multiple CCS plants will operate. By integrating atmospheric dispersion analysis with biogeochemical modelling of rivers and aquifers, this benchmark study highlights that millions of people and large protected areas in North-Western Europe may be impacted or repeatedly exposed to overlapping emissions. The novelty lies in a new framework combining industrial process data on plant capacity with environmental modelling, providing tools to better quantify pollutant dispersion and fate. This represents a first step toward stronger integration between engineering, atmospheric and environmental science. The findings highlight the need for harmonized modelling approaches, regulation, regional-scale risk assessment, and improved monitoring to ensure CCS activities remain safe while contributing to climate neutrality. By advancing approaches to assess pollutant dispersion, this research supports both industry and policymakers in balancing climate mitigation with water security and public health.

## 1. Introduction

The European Union's (EU) ambitious goal to achieve net-zero greenhouse gas (GHG) emissions by 2050 necessitates the

widespread implementation of carbon capture storage and reuse (CCSU) technologies.<sup>1,2</sup> Practically all IPCC emission scenarios rely heavily on CO<sub>2</sub> capture (CC) technologies to limit warming to 2 °C.<sup>3</sup> In the EU, net CO<sub>2</sub> removal should reach at least 50 Mton per year by 2030 and 250 Mton per year by 2050.<sup>2</sup> Among CC, amine-based CC is one of the most prevalent approaches due to its maturity for industrial use<sup>4,5</sup> and low cost, equipment demands and relatively low environmental footprint.<sup>6</sup> It has proven successful with a few retrofitted full-scale capture plants.

<sup>a</sup> Norwegian Institute for Water Research (NIVA), Økernveien 94, 0579 Oslo, Norway. E-mail: francois.clayer@ngi.no

<sup>b</sup> Norwegian Geotechnical Institute (NGI), Sandakerveien 140, 0484 Oslo, Norway

<sup>c</sup> NILU, Instituttveien 18, 2007 Kjeller, Norway



A key concern with amine technology is the dispersion of amines as well as carcinogenic nitrosamines (NSAs) and nitramines (NAs) into surface and groundwater, posing a critical human health risk.<sup>7</sup> These compounds form in the air during degradation of volatile amines emitted by the CC plant with the treated flue gas.<sup>8,9</sup> This reaction occurs rapidly (within minutes), generating NSAs and NAs whenever atmospheric oxidants (such as hydroxyl radical OH<sup>\*</sup>) and nitrogen oxides (NO<sub>x</sub>) are present.<sup>10,11</sup> The fact that these substances form in the atmosphere complicates the accurate prediction of their formation and deposition rates, as several complex physical and chemical processes must be considered.<sup>7</sup> In addition, many nitrosamines undergo rapid photodegradation under UV irradiation, whereas nitramines are far more photostable.<sup>12,13</sup> Given their persistence and potential to reach surface and groundwater, these byproducts may threaten critical drinking water sources across Europe, posing significant public health concerns.<sup>14,15</sup> In addition, NAs and NSAs, being water-soluble compounds,<sup>16</sup> can enter the food chain through contaminated irrigation and rainwater affecting water-rich crops such as fruits and vegetables.

Norway has set recommended safety limits for the sum of NSAs and NAs at 4 ng L<sup>-1</sup> in drinking water and 0.3 ng m<sup>-3</sup> in air which are enforced locally when issuing amine emission permits.<sup>17,18</sup> The values represent a minimal additional lifetime risk of cancer (10<sup>-6</sup> and 10<sup>-5</sup>, respectively). These risk estimates are based on the most potent nitrosamine, *N*-nitrosodimethylamine (NDMA). In contrast, NSAs and NAs are not specifically listed in the European Union's Drinking Water Directive, allowing individual EU member states to establish their own safety limits for these compounds. In Germany, for example, a health-based control limit of 10 ng L<sup>-1</sup> for NDMA in drinking water has been established by the Umweltbundesamt.<sup>19</sup> In the Netherlands, this limit is set at 12 ng L<sup>-1</sup>.<sup>20</sup> While some countries have set specific limits, most EU countries do not regulate these compounds explicitly, such as Belgium, reflecting the absence of EU-wide standards. However, the 4 ng L<sup>-1</sup> Norwegian limit and 10 ng L<sup>-1</sup> for NDMA are often used as references in risk assessments.<sup>7,21</sup> Other environmental limits can also be considered for wet ecosystems, although they are typically higher but consider only specific compounds and not the sum of NA and NSA.

NSAs and NAs can also originate from amines of both natural and anthropogenic sources.<sup>22,23</sup> In megacities such as London and Seoul, concentrations of NSAs and NAs were found to exceed the Norwegian safety limit with up to three orders of magnitude.<sup>24,25</sup> Daily concentrations in air (PM<sub>2.5</sub>) in Seoul were shown to span 0.06–54.72 ng m<sup>-3</sup> for NSAs and 0.08–2.40 ng m<sup>-3</sup> for NAs.<sup>26</sup> Similarly, concentrations of NSAs (15–26 ng L<sup>-1</sup>) above the safety limit have been found in water draining a mixed industrial, urban and agricultural area,<sup>27</sup> and occasionally NSAs and NAs have been found at high levels in drinking water and chlorinated swimming pools.<sup>28,29</sup> These findings underscore the limited understanding of existing sources of NSAs and NAs in the environment. With CC emerging as a potential new emission source, it is crucial to develop

robust tools for estimating NSA and NA pollution from amine-based CC. Such tools are essential to distinguish CC-related emissions from background pollution and to enable more accurate and equitable source attribution.

Within the EU, more than half of the CC projects are planned to be implemented along the south coast of the North Sea, from Northern France through Belgium, Netherlands, Northern Germany and Denmark.<sup>2</sup> This region, hereafter referred to as the “Franco-Danish Corridor” (Fig. 1), is becoming a key hub for CCS due to its high industrial emissions, proximity to offshore CO<sub>2</sub> storage sites, and well-developed infrastructure. The region's industrial clusters, including those in Rotterdam and Antwerp, contribute significantly to CO<sub>2</sub> emissions, making CCS crucial for decarbonization. Supported by governmental policies and investments, this region plays a central role in Europe's efforts to meet climate goals and achieve net-zero emissions. However, this region also faces water stress due to climate change impacts like droughts, flooding, and sea-level rise and high extraction rates.<sup>30</sup> While these areas are not traditionally water-scarce, there are several challenges related to water resources management for agricultural, industrial, and domestic use, particularly in low-lying regions like the Netherlands.<sup>31</sup> Coastal areas also face increased risks of flooding, making water management a critical issue in the region.

As Europe advances CC implementation, the widespread deployment of amine-based technologies necessitates a comprehensive regional assessment to understand their cumulative environmental and health impacts.<sup>32,33</sup> Current permitting processes predominantly address single-point emissions,<sup>34</sup> which fail to capture the broader implications of large-scale CC implementation. This gap highlights the need for a more holistic approach for regulatory frameworks. Additionally, regional assessments are crucial to evaluate the interaction of these technologies with local ecosystems and communities, ensuring sufficient access to natural resources and ecosystem services such as clean air, land availability, provision of drinking water, and energy.<sup>35</sup>

Given the potential health risks associated with NAs and NSAs, and the analytical challenges for their detection in environmental samples, it is crucial to develop robust models that can predict their concentrations in water resources. Such models can aid in assessing the impact of CC activities on water quality and comply with amine emission permits set to protect nearby drinking water sources against exceeding the NSA and NA safety limit. This paper first presents a dataset on CC implementation in Central EU, mainly within the Franco-Danish corridor, with a focus on amine-based CC projects. In addition, a catchment model capable of predicting the concentrations of NAs and NSAs in surface waters and groundwaters is used for two case studies in the region taken as theoretical examples. The model results highlight the influence of some key environmental parameters and processes on NAs and NSAs concentrations. We further discuss how the model tools can support the sustainable management of water resources in the context of increased CC implementation.





Fig. 1 Location map of the amine-based and other technology CC projects by 2030, water exploitation index (WEI) in river basin districts and 2019 NO<sub>x</sub> emissions (adapted from ref. 36) across the Franco-Danish corridor. The blue star and blue dotted line indicate the groundwater and surface water case-study, respectively. The green triangles within green squares amine-based CC projects indicate CC projects for which technology is currently unknown but highly likely to be amine-based.

## 2. Material & methods

### 2.1. CC projects dataset

A list of CC projects publicly announced across the Franco-Danish corridor was gathered through literature review and targeted web searches, including artificial intelligent assisted searches. Parameter values for the CC technology, tons CO<sub>2</sub> captured per year (by 2030 and by 2050), tower height and flue gas temperature for the identified CO<sub>2</sub> capture projects have been searched online using Google, Google Scholar, and Microsoft Copilot. The temperature of the emitted flue gas and the height of the absorber tower are two important parameters for predicting the atmospheric dispersion and ground deposition of amines, nitrosamines, and nitramines.<sup>32</sup> Search words included the project names or operator in combination with keywords like “CO<sub>2</sub> capture technology”, “absorber height”, “stack height”, “flue gas temperature”, “technical description”, *etc.* Exact parameter values for stack height and flue gas temperature were only successfully retrieved for 8 projects. For the remaining, parameter values have been estimated based on information available for similar categories of CO<sub>2</sub> emitters. Types of sources of information covered company homepages, press releases, applications for emission permits, Best Available Technology (BAT), reports, and peer-reviewed journal articles.

The quantities of CO<sub>2</sub> planned to be captured in each project were also validated against estimations from ref. 2. For 13 planned CC projects, the information on CC technology was not available. For these projects, we assumed that the technology was

amine-based only if the owner/operator is known to have other projects with amine technology and if the nature of the plant was compatible. Out of the 13 projects, 5 were marked as likely based on amine technology, representing about 3% of total CC capacity by 2030 in the dataset. In addition, 3 other projects were kept as potential sites for amine technology representing 14% of total CC capacity by 2030.

Total CC capacity by 2050 in the EU should reach a minimum of 250 Mton CO<sub>2</sub> per year.<sup>2</sup> Most existing and planned CC projects in the EU are along the Franco-Danish corridor, located in the study area. The conservative assumption that 50% of EU minimum target of 250 Mton CO<sub>2</sub> per year will be captured within the study area, *i.e.*, 125 Mton CO<sub>2</sub> per year, was used to scale up the total CC capacity in the region. Since it was not possible to include future new projects, existing projects (or planned projects) were assumed to be scaled up with no additional new projects.

### 2.2. Landscape characteristics

Landscape characteristics were aggregated by river basin districts as defined by EEA.<sup>37</sup> The Water Exploitation Index (WEI) is a measure of pressures on renewable water quantity within a river basin district over a season or a year due to human water usage.<sup>38,39</sup> WEI and data on population for each season were gathered by river basin districts from the EEA Rest ArcGIS services.<sup>40</sup> When WEI > 20%, water resources are considered stressed; WEI > 40% indicate severe stress and unsustainable use of freshwater resources.<sup>38</sup> Monthly NO<sub>x</sub> emissions at a



resolution of  $0.2^\circ \times 0.2^\circ$  were used and aggregated over each river basin district from satellite based  $\text{NO}_2$  observations over Europe.<sup>41</sup> We used  $\text{NO}_x$  emissions estimated by Van der A *et al.* (2024) using the Daily Emissions Constrained by Satellite Observations (DECSO) inversion algorithm applied to  $\text{NO}_2$  observations over Europe from the TROPOMI instrument<sup>42</sup> on board the Sentinel-5 Precursor (S5P) satellite. The extent area of Natura 2000 protected sites was retrieved from EEA Rest API services.<sup>40</sup> The gridded dataset on irrigated crop areas in Europe<sup>43</sup> was also used to estimate the total surface area of fruit and vegetable crops in the study region.

To estimate the population and land area potentially impacted by CC activities in the region of interest, an area of influence was calculated for each CC project based on the intensity of CC and dominant wind directions. Raster population density data was taken from.<sup>44</sup> Wind direction data was downloaded for each site from ERA5 data from the Copernicus Climate Data Store over 2000–2020<sup>45</sup> and the frequency of downwind direction for each cardinal and intercardinal direction was calculated. The main downwind direction represented at least 20% advocating for setting distinct distance of influence for each direction. Based on deposition rates used in previous studies,<sup>7,46</sup> the deposition of NA and NSA is highest within a 20-km radius of a small CC plant ( $<0.5$  Mton  $\text{CO}_2$  per year). For small plants, 20 km was thus taken as the maximum distance of influence for the dominant downwind direction. Under the least frequent downwind direction, the distance of influence was set to 7 km, and for the other downwind directions, the distance of influence was scaled linearly to wind frequency between 7 and 20 km. To account for the impact of different plant sizes, the distances of influence were multiplied by 2 and 3 for intermediate (0.5 Mton  $\text{CO}_2$  per year – 1 Mton  $\text{CO}_2$  per year) and large ( $>1$  Mton  $\text{CO}_2$  per year) CC plants, respectively. The resulting area of influence for a given CC plant was a combination of 8 octants for each wind direction with radiuses between 7 and 20 km, 14 and 40 km or 21 and 60 km for small, intermediate and large CC plants, respectively. Even though flue gas temperature and stack height can influence atmospheric dispersion,<sup>47–49</sup> the current approach consider that the area of influence depends only on plant capacity because of the lack of consistent data.

When reporting population and areas that are affected by CC activities, a distinction is made whether the population and

areas are affected by one or several CC plants. *Impacted population and area* refer to the distinct population or area within the influence of at least one CC plant. Each unit is counted once, regardless of whether it is affected by multiple CC plants. This metric therefore represents the unique footprint of CC activities on surrounding populations and areas. In contrast, *potential exposure* refers to the cumulative exposure count (*i.e.*, it accounts for the load), in which entities are counted multiple times if they fall within the influence zones of more than one CC plant. This metric captures the burden of overlapping exposures and reflects the intensity of potential risk in regions where multiple CC facilities operate.

### 2.3. NA and NSA deposition and amine solvents

To estimate NSA and NA deposition in the zone of influence of CC plants using four different solvents, we used a simplified scaling approach based on published amine emission data and solvent specific NSA and NA yields.

The composition of the amine solvent for CC is often restricted information since many technology providers develop their own solvent. Here we selected three common solvents and included one mixture: monoethanolamine (MEA;  $\text{C}_2\text{H}_7\text{NO}$ ), 2-amino-2-methyl-1-propanol (AMP;  $\text{CH}_3\text{C}(\text{NH}_2)(\text{CH}_3)\text{CH}_2\text{OH}$ ), piperazin,1,4-diazacyklohexan (PZ;  $\text{C}_4\text{H}_{10}\text{N}_2$ ) as well as CESAR1, a mixture of 2/3 AMP and 1/3 PZ by mass (*e.g.*<sup>50</sup>). MEA is known to have an extremely low potential to form NSAs and a low potential for NAs. It is thus considered the most environmentally friendly amine solvent used for CC. AMP and PZ are strongly considered for amine-based CC, separately or as mixtures, such as the CESAR1 solvent developed at Test Centre Mongstad (*e.g.*<sup>50</sup>). Selected atmospheric parameters for MEA, AMP and PZ are given in Table 1. PZ has a large potential to form NSA and NA. Calibration experiments performed by Tan *et al.* (2021) established the yield of NA to be 6% after 10 min and 7% after 30 min of reaction in their experiment. The maximum amount of NSA was found to be 9% of reacted PZ after 10 min dropping to 1% after 30 min because of photolysis and decreasing NO content during the experiment.

To estimate NA and NSA deposition for MEA, we adopted emission factors from,<sup>51,52</sup> representing a standard configuration with water wash and yielding average emissions of  $220 \text{ mg Nm}^{-3}$  for a 2.2 kt  $\text{CO}_2$  per year capture plant. Emissions

Table 1 Selected atmospheric parameters related to MEA, AMP and PZ atmospheric degradation to NA and NSA

Solvent	Parameter	Value ([range])	Ref.
MEA	Rate coefficients at 295–300 K for reaction with OH radicals	$k_{\text{OH}} = 7.02 \times 10^{-11} \text{ cm}^3 \text{ molecules}^{-1} \text{ s}^{-1}$	55 and 89
	Lifetime midday (OH concentration $C_{\text{OH}} = 10^6 \text{ molecules cm}^{-3}$ )	$\sim 4 \text{ h}$	
	NSA formation yield	0.01% [ $<0.02\%$ ]	90
	NA formation yield	1.9% [1–2%]	55
AMP	Rate coefficients at 295–300 K for reaction with OH radicals	$k_{\text{OH}} = 2.8 \times 10^{-11} \text{ cm}^3 \text{ molecules}^{-1} \text{ s}^{-1}$	91
	Lifetime midday (OH concentration $C_{\text{OH}} = 10^6 \text{ molecules cm}^{-3}$ )	$\sim 10 \text{ h}$	
	NSA formation yield	2.3% [0.6–2.3%]	92
	NA formation yield	8.9% [8–9%]	55
PZ	Rate coefficients at 295–300 K for reaction with OH radicals	$k_{\text{OH}} = 2.8 \times 10^{-10} \text{ cm}^3 \text{ molecules}^{-1} \text{ s}^{-1}$	93
	Lifetime midday (OH concentration $C_{\text{OH}} = 10^6 \text{ molecules cm}^{-3}$ )	$\sim 1 \text{ hr.}$	
	NSA formation yield	9.0% [1–12%]	93 and 94
	NA formation yield	7.0% [6–7%]	93



for AMP, PZ, and the CESAR1 blend were derived from,<sup>53</sup> who reported 56 mgNm<sup>-3</sup> AMP and 30 mgNm<sup>-3</sup> PZ for a similarly sized plant with a mixed solvent similar to CESAR1. These values were scaled to emissions of 84 mgNm<sup>-3</sup>, 90 mgNm<sup>-3</sup> and 86 mgNm<sup>-3</sup> for AMP, PZ and CESAR1 solvents, respectively, consistent with the ranges reported by<sup>54</sup> for emissions following water-wash. NA and NSA formation was then estimated by applying the solvent-specific yields in Table 1 along with molecular mass conversion factors of 1.3–1.7.<sup>11</sup> Following,<sup>55</sup> we assumed that 90% of emitted degradation products deposit within the defined zone of influence (8 octants; see above), decreasing linearly from the stack and following an atmospheric concentration ratio of 5 between the source and the zone boundary (maximum distances of 20, 40, and 60 km for small, medium, and large domains). For surface-water (river) deposition, we further assumed 50% photolytic degradation of NSA in the atmosphere or water column in line with,<sup>7</sup> while only 20% removal was applied for groundwater due to limited sunlight exposure. Photolysis plays a minor role for MEA emissions, for which ~95% of degradation products are nitramines, whereas PZ produces a much higher proportion of nitrosamines (>50%), making photolysis more relevant for PZ-based solvents. Case-study unconfined groundwater.

In the EU members states, 65% of the urban drinking water is coming from groundwater<sup>30</sup> with about 40% and 65% for Belgium and the Netherlands, respectively,<sup>31</sup> making it a valuable resource. Small unconfined sandy aquifers are common in the North Sea region (Belgium, Netherlands, Germany, Denmark and Sweden;<sup>56</sup>). As a representative case of these aquifers, we selected the Sint Jansteen sub-aquifer (Fig. 1; 51.247°N, 4.057°E), part of the larger NLGWSC0002 aquifer in the Netherlands, spanning 15–20 km<sup>2</sup>.<sup>57</sup> This unconfined sand aquifer, where water extraction has been active since 1936, is primarily used for industrial water extraction but also serves as a backup drinking water source. The aquifer, 10–15 meters thick, allows for an annual extraction of up to 3.0 Mm<sup>3</sup>, though actual extraction averages 2.8 Mm<sup>3</sup> per year. Recent analyses indicate that the aquifer's water quality has faced challenges, and travel time studies suggest a residence time of 5 to 15 years for various chemical compounds.

The Sint Jansteen aquifer is representative of small, unconfined, sandy aquifers that are common throughout the Belgian–Dutch–German region.<sup>56</sup> Similar systems—such as coastal dune sands, paleo-tidal channels, and Quaternary sandy deposits—occur widely in Belgium's Flemish coast and in the Netherlands (Zeeland, Noord-Brabant;<sup>58,59</sup>), as well as in northern Germany where glaciofluvial and coastal sandy aquifers display comparable hydrogeological properties.<sup>60,61</sup> Comparable behaviour is also observed in inland unconfined sands such as the Brusselian Sands aquifer,<sup>62</sup> which exhibits small recharge zones and travel times ranging from months to a few decades.<sup>63</sup> Overall, these similarities indicate that Sint Jansteen provides a realistic analogue for assessing NA + NSA transport in many unconfined sandy aquifers across the Franco-Danish corridor.

## 2.4. Case-study surface water

Surface water also contributes significantly to drinking water production in the EU (35%,<sup>30</sup> with about 60% and 35% for Belgium and the Netherlands, respectively.<sup>31</sup> As a representative theoretical case of surface water, we selected the upper part of the Schelde catchment<sup>64</sup> covering 5200 km<sup>2</sup> across Northern France and Belgium, upstream of the discharge station Helkijn (Fig. 1; 50.729°N, 3.388°E; No# 6220204 from ref. 65). Although the Schelde river is not used for drinking water, it is a representative site for the nearby catchments, including the Meuse River supplying over 7 million inhabitants with drinking water (514.5 Mm<sup>3</sup> in 2020;<sup>66</sup>). The Meuse River could not be easily modelled because of complex regulation patterns (abstraction, storage, retention;<sup>67</sup>).

## 2.5. Surface and ground-water modelling

The semi-distributed catchment model SimplyTox,<sup>68</sup> applied to both the surface and groundwater cases, is a simplification of INCA-Contaminant.<sup>7,69</sup> SimplyTox simulates NA and NSA transportation through soil- and groundwater and river runoff accounting for evapotranspiration, biodegradation in soil and groundwater as well as NA and NSA partitioning between water, air, solid and dissolved organic carbon. Key physio-chemical parameters for NA and NSA such as the enthalpy of phase transfer between air and water were taken from ref. 7 (see Table S1). Biodegradation of NAs and NSAs follows a simple exponential decay with a temperature-adjusted rate, 5% rate change per 1 degree change in temperature (equivalent to a Q10 of 1.63;<sup>46</sup>). Biodegradation half-life values are given for 8 °C.

For the surface water case, the catchment was represented as a semi-distributed river network with associated catchment area and shallow and deep soil connected to the river reach. Subcatchment hierarchy including catchment area, river slope and length was described by the hydrobasins level 12.<sup>70</sup> The model is driven by daily air temperature and precipitation (ERA5 from 1990 to 2023;<sup>45</sup>) downloaded separately for each sub-catchment through the Open-Meteo API,<sup>71</sup> and constant NA + NSA deposition rates. The surface case was then auto calibrated, following,<sup>68</sup> over 2005–2022 against daily discharge from the Helkijn station. In addition, the sensitivity of long-term NA + NSA concentration in the river, *i.e.*, the mean concentrations after a few years when the river has reached equilibrium, to main hydrological parameters, *i.e.*, baseflow index, soil field capacity, soil and groundwater time constants, was estimated.

For the groundwater case, the aquifer was represented as a layered basin (thirty 1-m thick layers with a variable water content) with a fixed abstraction rate (2.8 Mm<sup>3</sup> per year; ref) at the lowermost box and a variable infiltration rate based on soil water content and scaled to sustain a stable groundwater level with realistic seasonal and yearly variations (see Fig. S1). The water capacity of the groundwater layers was calibrated to obtain the desired average travel time (*i.e.*, 5 or 10 years) given the infiltration and extraction rates.

A range of realistic NA + NSA deposition rates of 0 to 15 ng m<sup>-2</sup> day<sup>-1</sup> was taken from recent environmental assessments of small CC plants (0.5 to 1 Mton CO<sub>2</sub> per year;<sup>7,32,46</sup>) as input for both cases. In addition, the deposition estimated for



each solvent, as described in Section 2.2 above, were used to run a sensitivity analysis assessing the impact of solvent type and downwind distance to the amine-based CC plant on equilibrium NA + NSA concentration in surface and groundwater.

### 3. Results & discussion

#### 3.1. Amine-based technologies dominate CC ramping towards 2050

The 45 planned CC projects located within the Franco-Danish corridor (Fig. 1) will have a combined CC capacity of 46.2 Mton

CO<sub>2</sub> per year by 2030 (Fig. 2a). Considering that EU CC capacity will reach 58.9 Mton CO<sub>2</sub> per year by 2030,<sup>2</sup> 79% of the capacity within the EU would be located within the Franco-Danish corridor and 60% in Belgium and the Netherlands alone. Within the Franco-Danish corridor, at least 43% of the capacity will be based on amine technologies, *i.e.*, 20.0 Mton CO<sub>2</sub> per year. For 37% of the announced CC capacity, the technology is unknown, but this includes 3% and 14%, respectively, that are very likely and possibly amine-based considering the experience and in-house expertise of the plant owners (Fig. 2a). The CryoCap<sup>®</sup> technology, based on cryogenic gas separation,<sup>72</sup> will represent 6% of the capacity while each of the other



Fig. 2 Projections of CC capacity by technology in the Franco-Danish corridor over 2025–2050 (a) and population under water stress (b) and severe water stress (c) over 1990–2015 in the 11 river basin districts (see Table 2) and proportion of population expected to be impacted by NAs and NSAs pollution.



technologies, such as calcination,<sup>73</sup> oxyfuel,<sup>73</sup> alkali absorption,<sup>74</sup> HISORP<sup>®75</sup> and carbonate fuel cells<sup>76</sup> will be implemented in less than 4%. Further assuming that the Franco-Danish corridor would host about 50% of EU's CC capacity by 2050, at least 50 Mton CO<sub>2</sub> per year would be captured with amine technology in the region, and at least 36.5 Mton CO<sub>2</sub> per year in Belgium and the Netherlands alone.

The widespread planned implementation of amine-based technologies is consistent with the fact that this technology is more mature, commercially viable and more easily retro-fitted to existing CO<sub>2</sub> emissions sites compared to other technologies.<sup>6</sup> In addition, the amine supply chain is well developed in the EU with more than 4 Mtons of amine produced in 2023 and a 5% expected annual growth towards 2033.<sup>77</sup> Considering an amine requirement of maximum 1.0 kg per tonCO<sub>2</sub>,<sup>78</sup> additional production of 0.1–0.2 Mton per year of amine would likely be sufficient to sustain 2050 amine-based CC in the EU. In contrast, other technologies still require material optimization and implementation of streamlined industrial processes to decrease costs and equipment space requirements.<sup>79</sup> Amine-based materials have proven to be useful and polyvalent in CC and CO<sub>2</sub> utilization, but several challenges related to cost and regeneration remain to be overcome before they can be widely and rapidly expanded.<sup>80,81</sup>

### 3.2. Environmental risks for drinking water, natural reserves and crops

The Franco-Danish corridor is densely populated and hosts numerous Natura 2000 reserves covering 19 700 km<sup>2</sup> in Belgium

and the Netherlands, alone. Vegetable and fruit crops are also abundant in this region with 25 650 ha cultivated across the two countries.<sup>43</sup> By 2030, Belgium and the Netherlands will account for 60% of the CC capacity, but only the Netherlands have planned to widely develop amine technology (Table 2). The potential area impacted by amine-based CC plants within the Franco-Danish corridor spans 33 600 km<sup>2</sup>, with nearly 20% (6365 km<sup>2</sup>) falling within Natura 2000 reserves and hosting about 15.2 million inhabitants. A significant portion of this area will be impacted by two or more plants, especially in the Netherlands. Accounting for multiple exposures, the total surface area exposed is 43 950 km<sup>2</sup> of which 9520 km<sup>2</sup> of natural reserve.

In line with high CC activities, the Netherlands shows the highest potential for human exposure to NAs and NSAs. Potential human exposure does not scale linearly with CC capacity because of large transnational exposure. For example, potential human exposure is lower in France than in Germany due to the dominant North-East downwind direction in the region and despite larger amine-based CC capacity in France (Table 2). Similarly, Natura 2000 reserves exposure in Belgium and Germany are potentially caused by NAs and NSAs from France and the Netherlands, respectively. Regarding vegetable and fruit crops, all exposure is due to domestic emissions, except for Belgium which is a net receiver of French NAs and NSAs emissions.

Water scarcity is widespread across Europe, up to 70% of the population of several countries can be under water stress in summer.<sup>30</sup> In the densely populated Franco-Danish corridor,

**Table 2** Impacts of amine-based CC capacity in 2030 on population, Natura 2000 reserves and vegetable/fruits crops as well as potential exposure by country. The CC capacity ranges in Belgium and the Netherlands are due to uncertainty in the technology for 3 of the announced CC projects. Potential exposure refers to the cumulative exposure in which entities are counted multiple times if they fall within the influence zones of more than one CC plant. n.a.: not applicable

Country	Belgium	Denmark	France	Germany	Netherlands	Total
Amine-based CC capacity (Mton CO <sub>2</sub> year <sup>-1</sup> in 2030)	1.1–3.1	2.1	2.2	1.1	13.5–18.0	20.0–26.5
Other CC capacity (Mton CO <sub>2</sub> year <sup>-1</sup> in 2030)	11.5–13.5	0.4	3.2	2.1	2.7–7.2	19.9–26.4
Human potential exposure (10 <sup>6</sup> capita)	1.9	2.3	1.1	3.0	12.2	20.5
Population impacted (10 <sup>6</sup> capita)	1.6	1.5	0.9	2.7	8.5	15.2
Fraction impacted of national total (%)	14	28	1	3	51	n.a.
Origin of impact (%):						
Belgium	89		8		3	
Denmark		100				
France	5		92			
Germany				83		
Netherlands	6			17	97	
Natura 2000 reserves potential exposure (km <sup>2</sup> )	863	1716	1461	2870		6910
Natura 2000 reserves impacted (km <sup>2</sup> )	607	1396	967	1605		4575
Fraction impacted of national total (%)	14	7	1	3		n.a.
Origin of impact (%):						
Belgium	23		1		22	
Denmark		100				
France	76		99			
Germany				5		
Netherlands	1			95	78	
Potential vegetable/fruit crops exposure (ha)	842	283	1242	364	8490	11 221
Vegetable/fruit crops impacted (ha)	842	276	910	364	7134	9526
Fraction impacted of national total (%)	19	26	0.5	1	34	n.a.
Origin of impact (%):						
Belgium	53				14	
Denmark		100				
France	47		100			
Germany				100		
Netherlands					86	



agriculture, industries, public water supply, and tourism contribute to water stress (Fig. 1;<sup>30</sup>). The highest potential human-, Natura 2000 and crops exposure to NAs and NSAs often co-locate with river basin districts showing high WEI values (Table 3). In particular, the Meuse, Zealand and Rhine Coastal: Lek districts show high average WEI values and strong potential for NAs and NSAs exposure. A total of 68.5 million people is living within the 11 river basin districts where amine-based CC plants will be located. Among these, up to 32 million people have been under water stress (WEI > 20), and up to 20 million have been under severe water stress (WEI > 40) regularly over 1990–2015 (Fig. 2b and c). A significant part of the population, up to 10.7 and 9.2 million inhabitants for intermediate and severe water stress respectively, will be also exposed to potential NAs and NSAs pollution (Fig. 2b and c).

Placing a CC plant within 100–200 km downwind of existing plants will likely lead to flue gas plume interferences.<sup>32</sup> Amines and potentially NO<sub>x</sub> from neighboring plants will likely result in positive feedback on the production rates of NAs and NSAs. The potential interference between flue gas plumes suggests that the current preliminary estimate of the area of influence of amine-based CC plants, based on the upscaling of isolated point source studies, is likely conservative. Additionally, we assumed that no new CC plant would be established after 2030, with only existing sites being scaled up by increasing their CC capacity. However, among the top 100 industrial GHG emitters in the EU – responsible for nearly 40% of industrial GHG emissions<sup>82</sup> – several key sites in Germany, Poland, and Southern Europe are not adequately represented in our dataset. While considering sites in Southern Europe falls outside the scope of this study, the Rhine-Ruhr region in Germany and the Germano-Polish region, spanning from Brandenburg to Łódź, host several of the top 10 industrial sites in the EU, emitting between 10 and 37 MtCO<sub>2</sub> per year.<sup>82</sup> These regions would represent additional areas of concern, potentially increasing the regional load of NAs and NSAs in the Franco-Danish corridor upon the implementation of amine-based CC. These limitations underscore the need for advanced model tools to

better predict environmental impacts of multiple amine-based CC plants within a given region.

### 3.3. Modelling concentrations in surface and groundwater

Catchment modeling is essential to estimate the NAs and NSAs concentrations in surface and groundwater resulting from the complex interactions between hydrological and biogeochemical processes.<sup>7</sup> While some specific NAs and NSAs are known to undergo biodegradation, considerable uncertainty remains regarding the biodegradation potential of most of NAs and NSAs with several compounds expected to persist in the environment.<sup>83,84</sup> In contrast, rapid photodegradation of NSAs has been established.<sup>12,13</sup> Here, a catchment model was set up for the upper Schelde River upstream of Helkijn station. Following calibration, the daily discharge was accurately simulated with Nash–Sutcliffe (NSE) and Kling–Gupta efficiencies (KGE) of 0.5 and 0.65, respectively (Table S2 and Fig. S2<sup>85</sup>). In addition, a groundwater model was set up for a shallow unconfined aquifer to reproduce seasonal and long-term variations in water storage (Fig. S1). Both applications were used to estimate the impact of NA + NSA deposition and NA + NSA half-life on equilibrium concentrations in the river or the aquifer (Fig. 3). In the river case, equilibrium concentrations show mainly sensitivity to NA + NSA deposition, while NA + NSA half-life only has significant influence when half-life is below 2 years (Fig. 3a). In contrast, in the aquifer case, the NA + NSA half-life has a strong influence on the equilibrium concentrations (Fig. 3b and c), especially when the water travel time is longer (Fig. 3c). Consistently, the river equilibrium concentrations show little sensitivity to hydrological parameters (Fig. 4) while the groundwater equilibrium concentrations are sensitive to the travel time (Fig. 5). In fact, in the river, the travel time, governed by the baseflow index, soil and groundwater time constants, being below 2 years, is short compared to most of NA + NSA possible half-lives. Biodegradation has thus a limited impact on equilibrium concentrations because of time constraints. In the aquifer case, the travel time range overlaps with the NA + NSA half-life range creating highly sensitive conditions for NA + NSA equilibrium concentrations (Fig. 3b, c and 5).

**Table 3** Impacts of amine-based CC capacity in 2030 on population, Natura 2000 reserves and vegetable/fruits crops as well as potential exposure by river basin district. Countries are ranked following decreasing area coverage or number of capita. FR: France, BE: Belgium, DK: Denmark, NL: Netherlands and DE: Germany

River basin districts	District code	Countries	Mean WEI	Impacts of amine-based CC plants					
				Human (10 <sup>6</sup> capita)		Natura 2000 (km <sup>2</sup> )		Crops (ha)	
				Exposure	Impact	Exposure	Impact	Exposure	Impact
Scheldt coastal	WSB0000445	FR/BE/NL	6	1.9	1.2	230	191	3582	2332
Schelde	WSB0000138	FR/BE/NL	22	1.1	1.0	147	147	502	502
Meuse	WSB0000304	FR/BE/NL	67	1.2	1.1	143	117	1882	1870
Seine main Low	WSB0000455	FR	4	0.5	0.5	16	20	60	59
Zealand	WSB0000633	DK	27	2.4	1.5	316	268	189	189
Jutland Atlantic	WSB0000202	DK	3	0.3	0.3	33	33	121	115
Ems	WSB0000135	DE/NL	18	0.8	0.5	200	142	64	63
Rhine main Low	WSB0000415	DE/NL	6	2.4	2.3	90	90	497	497
Main	WSB0000291	DE	6	0.1	0.1	77	77	6	6
Rhine coast: Lek	WSB0000414	NL/DE	39	9.7	6.6	400	400	4321	3865
Rhine coast: 1	WSB0000412	NL/DE	10	0.2	0.2	35	31	11	7



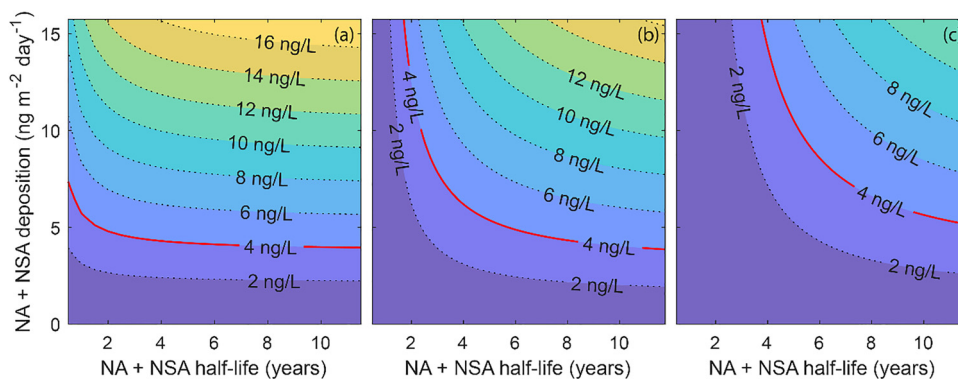


Fig. 3 Equilibrium NA + NSA concentration in the upper Schelde River (a) and a shallow unconfined aquifer (b): with water travel time of 5 years; and (c): with water travel time of 10 years) as function of NA + NSA deposition and NA + NSA half-life. The red line highlights the safety limit of  $4 \text{ ng L}^{-1}$ .



Fig. 4 Sensitivity of equilibrium NA + NSA concentration in the upper Schelde River (NA + NSA deposition rate:  $8 \text{ ng m}^{-2} \text{ day}^{-1}$ ) and NA + NSA half-life of 2 years) to main hydrological parameters: soil water time constant (a), baseflow index (b), soil field capacity (c) and groundwater time constant (d). Red vertical lines indicate calibrated parameter values used to produce Fig. 3a.

This sensitivity is particularly relevant for small unconfined sandy aquifers—such as those represented by our Sint Jansteen case study—where travel times typically span a few months to 10–15 years across catchments on the order of tens to hundreds

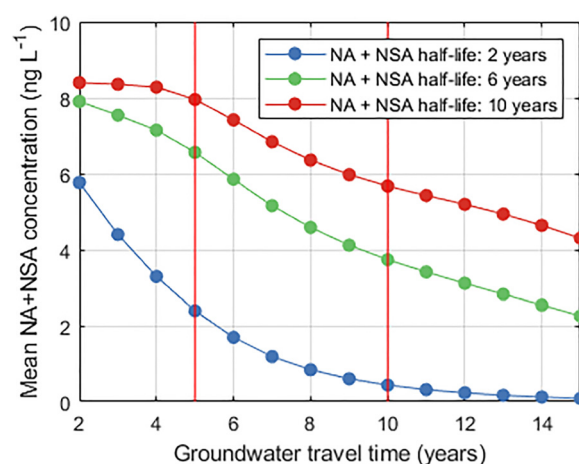


Fig. 5 Sensitivity of equilibrium NA + NSA concentration in a shallow unconfined aquifer (NA + NSA deposition rate:  $8 \text{ ng m}^{-2} \text{ day}^{-1}$ ) to groundwater travel time for different NA + NSA half-lives. Each red vertical line indicates the parameter value used to produce Fig. 3b and c, respectively.

of  $\text{km}^2$ . Such small, unconfined aquifers are common through Belgium, the Netherlands and Northern Germany (e.g.,<sup>58–61</sup>). Since our analysis focuses on equilibrium (rather than transient concentration evolution), we deliberately selected travel time as the primary governing parameter. While dilution capacity influences how quickly equilibrium is reached, the equilibrium level itself is controlled predominantly by the balance between travel time and degradation half-life. Parameters such as aquifer depth offer limited quantitative insight into this balance. Consequently, although the aquifer scenario produces more uncertain but generally lower equilibrium concentrations than the river system, it also exhibits substantially greater sensitivity to NA + NSA half-life due to the overlapping temporal scales of transport and decay.

This modelling exercise suggests surface waters with short residence times ( $<1\text{--}2$  years) are prone to NA + NSA concentration above the  $4 \text{ ng L}^{-1}$  Norwegian safety limit with relatively modest NA + NSA deposition rate ( $\sim 5\text{--}6 \text{ ng m}^{-2} \text{ day}^{-1}$ ).



While in shallow unconfined aquifers, the NA + NSA concentration is slightly more uncertain and depends on the interplay between groundwater travel time and NA + NSA half-life. Small systems are particularly at risk, where the low potential for dilution and short residence time for degradation create conditions for high NA + NSA concentrations.

### 3.4. Influence of the amine-solvent on NA + NSA concentration in water resources

The deposition values ( $5\text{--}15\text{ ng m}^{-2}\text{ day}^{-1}$ ) applied above represent a realistic range for relatively small CC plants with annual capacities of  $0.5\text{--}1\text{ Mt CO}_2$ . Comparable values and modelling set-ups have been used in permitting and impact assessments, where regional chemistry–transport models coupled to catchment fate models predict low  $\text{ng L}^{-1}$  drinking-water concentrations under realistic amine emissions, while emphasizing sensitivity to the biogeochemical processes and meteorology.<sup>7,32,46</sup> Under large scale deployment of amine-based CC, both the increased CC capacity and the possible plume interactions can become prominent sources of variability for NA and NSA concentrations in water resources.

Consistent with MEA's lower atmospheric yields of NSA and NA relative to several alternatives, our simplified scaling predicts the lowest equilibrium NA + NSA concentrations for MEA in both groundwater and river-basin downwind of a large CC plant (Fig. 6a and 7a). In contrast, despite lower parent-amine emissions for AMP, PZ, and CESAR1, their higher formation yields (Table 1)—particularly for PZ—lead to substantially

higher estimated equilibrium concentrations that are broadly similar across these solvents (Fig. 6b–d and 7b–d). These results should be interpreted as indicative since NSA + NA deposition was estimated using a simplified approach and detailed gas-phase chemistry, secondary aerosol formation, or explicit plume–plume chemistry is currently missing. We also adopt standard water-wash emission factors; while additional abatement (*e.g.*, acid wash, dry-bed) can significantly lower parent-amine emissions.<sup>54</sup> Other parameters, such as flue gas temperature and stack height, are expected to strongly influence dispersion and thereby deposition in the surrounding environment.<sup>47–49</sup> Although process optimization can reduce NA and NSA deposition, the expansion of CC facilities—including large, closely spaced plants ( $2\text{--}5\text{ Mt CO}_2$  per year; Fig. 1)—means that cumulative interactions may offset gains from individual optimizations, highlighting the need to assess combined impacts. Trade-offs between cost/chemical process complexity and residual emissions should be evaluated at both the plant scale and regional scales.

Under identical operational setups with water wash, MEA consistently yields lower modelled NA/NSA risks than AMP/PZ/CESAR1 (Fig. 6 and 7), reinforcing its status as a lower-risk baseline solvent for local water-quality objectives. However, considering the current limitations of our approach, future permitting should (i) require regional modelling that resolves NO<sub>x</sub> fields and multi-plume interactions, (ii) evaluate enhanced emissions controls (*e.g.*, acid-wash, dry-bed;<sup>54</sup>), and (iii) consider stack design/thermal buoyancy to manage near-field deposition



Fig. 6 Sensitivity of equilibrium NA + NSA concentration in a shallow unconfined aquifer to downwind distance to a large CC plant ( $1.5\text{ Mton CO}_2$  per year) for different NA + NSA half-lives following amine-based CC with different solvents: MEA (a), AMP (b), PZ (c) and CESAR1 (d). The red line highlights the safety limit of  $4\text{ ng L}^{-1}$ .



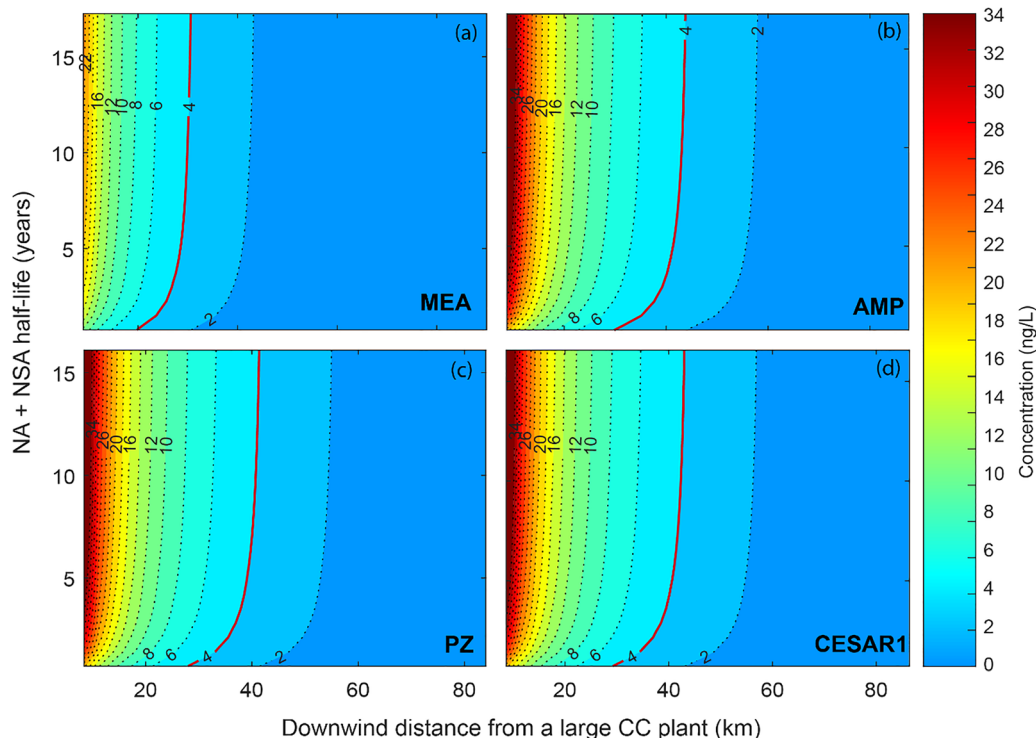


Fig. 7 Sensitivity of equilibrium NA + NSA concentration in a river basin (with soil water retention time of 8 days, groundwater retention time of 400 days and baseflow index of 0.75 similar to the Upper Schelde river basin) to downwind distance to a large CC plant (1.5 Mton CO<sub>2</sub> per year) for different NA + NSA half-lives following amine-based CC with different solvents: MEA (a), AMP (b), PZ (c) and CESAR1 (d). The red line highlights the safety limit of 4 ng L<sup>-1</sup>.

footprints.<sup>49</sup> Beyond simple proportional scaling with capacity, non-linear chemistry and plume dynamics at 1–5 Mt CO<sub>2</sub> year<sup>-1</sup> plants (and clusters thereof) can bias low first-order deposition estimates—both by increasing near-field oxidant and NO<sub>x</sub> availability, and by overlapping plumes that prolong NA and NSA production. These recommendations align with the need for advanced modelling tools and multi-compartment risk translation, from CC plant operational design, atmospheric dispersion modelling, deposition, and fate in surface- and groundwater<sup>86</sup> before consenting to large, clustered CC deployment and for Best Available Techniques (BAT) selection.

### 3.5. Implications of the heterogeneous EU regulation on transboundary emissions

The heterogeneous regulatory landscape across EU member states regarding NA and NSA emissions from amine-based CC creates pre-conditions for *trans*-boundary local water or environmental conflicts. Table 2 illustrates the multiple situations where *trans*-boundary issues can arise. Uneven national standards can cause shifting environmental burdens to downwind countries. For example, the Sint Jansteen aquifer in the Netherlands is already expected to receive an estimated ~10% of its NA + NSA deposition from emission sources in Belgium (Table 4); with continued industrial expansion around the Ghent hub (Belgium) this transboundary contribution could increase substantially. Notably, the Netherlands applies a much stricter drinking-water limit of 12 ng L<sup>-1</sup> for NDMA,<sup>20</sup> whereas

Table 4 Maximum estimated deposition for the Sint Jansteen aquifer (Netherlands) located 12 km, 18 km and 20 km downwind of one medium and two small size CC plants, respectively. Deposition is estimated using a simple scaling approach and including only water wash as emission abatement measure. About 10% of the deposition originates from Belgium

Solvent	Deposition (ng m <sup>-2</sup> day <sup>-1</sup> )		
	NA	NSA	Total
MEA	5.7	0.3	6.0
AMP	10.2	1.9	12.1
PZ	9.3	8.5	17.8
CESAR1	9.9	4.1	14.0

in Belgium the risk assessment for CC implementation would likely follow the WHO guideline value of 100 ng L<sup>-1</sup>.<sup>87</sup> These dynamics underscore the need for harmonized, *trans*-national regulation on NA and NSA to ensure that rapid CC deployment does not create unequal or unmanaged risks for shared air and water resources.

## 4 Conclusion

Amine-based technologies are projected to dominate carbon capture across the Franco-Danish corridor, with at least 20 Mton CO<sub>2</sub> per year captured by 2030. While their maturity and commercial viability make them attractive,<sup>6</sup> our analysis shows that widespread deployment poses significant risks to drinking



water (up to 15.2 million inhabitants impacted), Natura 2000 reserves, and agricultural crops. Belgium and the Netherlands, already experiencing chronic water stress, are especially vulnerable because of their high population density where several million people could be affected by emissions from multiple CC installations. While amine-based CC is mature and effective, it carries specific environmental risks as outlined here. In contrast, alternative technologies like the CryoCap<sup>®</sup> technology, solid sorbents or membrane systems generally reduce solvent-related emissions but introduce their own trade-offs, including material production impacts and higher energy demands.<sup>6</sup>

Using realistic deposition ranges (5–15 ng m<sup>-2</sup> day<sup>-1</sup>) representative of small CC plants (0.5–1 Mt CO<sub>2</sub> per year) as well as empirically estimated deposition, our modelling demonstrates that surface waters with short residence times are highly sensitive to deposition rates, whereas groundwater concentrations depend strongly on the interaction between NA + NSA half-lives and travel times. These dynamics make small aquifers especially vulnerable due to limited dilution capacity. Overall, MEA emerges as the lowest-risk solvent for nearby water resources, unless additional emission abatement measures are implemented (*e.g.*, acid-wash). Downwind distance remains a primary determinant of local risk in the present assessment. The deployment of multiple large CC plants is likely to introduce additional non-linear chemical interactions and plume-dynamic effects that could substantially modify future exposure and impact patterns.

Although emissions can be mitigated at the plant scale with several operational optimization methods,<sup>88</sup> the cumulative effects of several neighbouring CC facilities could markedly increase deposition and must be evaluated explicitly. Regional-scale models integrating dispersion, deposition, and hydrological fate are therefore indispensable. Without EU-wide safety limits for NAs and NSAs, adopting such tools is critical to keep overall risk at a manageable level as CC deployment accelerates.

## Author contributions

Conceptualization: FC, CBG, LP, TFB; Data curation: FC, CBG, ASG; Formal analysis: FC, MN; Funding acquisition: FC, CBG; Investigation: FC, CBG, ASG; Methodology: FC, CBG, ASG, MN, LP, TFB; Project administration: FC, CBG; Software: MN, FC; Validation: MN, FC, LP; Visualization: FC, LP; Writing – original draft: FC, CBG; Writing – review and editing: All.

## Conflicts of interest

There are no conflicts to declare.

## Data availability

All data presented in this manuscript is publicly available at <https://doi.org/10.4211/hs.5d42596fc99a43db80b5ea74a2924e8b>.

Supplementary information (SI) including river and ground-water model parameters and calibration statistics. See DOI: <https://doi.org/10.1039/d5ee07330h>.

## Acknowledgements

This study was supported by NIVA, NILU and NGI internal funding and the Norges Forskningsråd (NFR) FuNitr project (grant no. 336357). We thank Hans-Fredrik Veiteberg Braaten for early support and Heleen de Wit for assistance navigating through Dutch environmental reports.

## References

- 1 European Commission, Going climate-neutral by 2050: a strategic long term vision for a prosperous, modern, competitive and climate neutral EU economy, Publications Office of the European Union, 2019. Available from: <https://data.europa.eu/doi/10.2834/02074>.
- 2 D. Tumara, A. Uihlein and I. Hidalgo González, Shaping the future CO<sub>2</sub> transport network for Europe, Publications Office of the European Union, 2024. Available from: <https://data.europa.eu/doi/10.2760/582433>.
- 3 IPCC. AR6 Synthesis Report: Climate Change 2023, 2023. Report No. Available from: <https://www.ipcc.ch/report/sixth-assessment-report-cycle/>.
- 4 G. T. Rochelle, Amine Scrubbing for CO<sub>2</sub> Capture, *Science*, 2009, **325**(5948), 1652–1654, DOI: [10.1126/science.1176731](https://doi.org/10.1126/science.1176731).
- 5 M. Wang, A. Lawal, P. Stephenson, J. Sidders and C. Ramshaw, Post-combustion CO<sub>2</sub> capture with chemical absorption: A state-of-the-art review, *Chem. Eng. Res. Des.*, 2011, **89**(9), 1609–1624, DOI: [10.1016/j.cherd.2010.11.005](https://doi.org/10.1016/j.cherd.2010.11.005) Special Issue on Carbon Capture & Storage.
- 6 S. F. Chang, H. H. Chiu, H. S. Jao, J. Shang, Y. J. Lin and B. Y. Yu, Comprehensive evaluation of various CO<sub>2</sub> capture technologies through rigorous simulation: Economic, equipment footprint, and environmental analysis, *Carbon Capture Sci. Technol.*, 2025, **14**, 100342, DOI: [10.1016/j.cst.2024.100342](https://doi.org/10.1016/j.cst.2024.100342).
- 7 M. D. Norling, F. Clayer and C. B. Gundersen, Levels of nitramines and nitrosamines in lake drinking water close to a CO<sub>2</sub> capture plant: A modelling perspective, *Environ. Res.*, 2022, **212**, 113581, DOI: [10.1016/j.envres.2022.113581](https://doi.org/10.1016/j.envres.2022.113581).
- 8 C. Guedard, D. Picq, F. Launay and P. L. Carrette, Amine degradation in CO<sub>2</sub> capture. I. A review, *Int. J. Greenhouse Gas Control*, 2012, **10**, 244–270, DOI: [10.1016/j.ijggc.2012.06.015](https://doi.org/10.1016/j.ijggc.2012.06.015).
- 9 G. T. Rochelle, Thermal degradation of amines for CO<sub>2</sub> capture, *Curr. Opin. Chem. Eng.*, 2012, **1**(2), 183–190, DOI: [10.1016/j.coche.2012.02.004](https://doi.org/10.1016/j.coche.2012.02.004).
- 10 N. R. Choi, Y. G. Ahn, J. Y. Lee, E. Kim, S. Kim and S. M. Park, *et al.*, Particulate Nitrosamines and Nitramines in Seoul and Their Major Sources: Primary Emission versus Secondary Formation, *Environ. Sci. Technol.*, 2021, **55**(12), 12, DOI: [10.1021/acs.est.1c01503](https://doi.org/10.1021/acs.est.1c01503).



- 11 C. J. Nielsen, H. Herrmann and C. Weller, Atmospheric chemistry and environmental impact of the use of amines in carbon capture and storage (CCS), *Chem. Soc. Rev.*, 2012, **41**(19), 6684–6704, DOI: [10.1039/C2CS35059A](https://doi.org/10.1039/C2CS35059A).
- 12 L. Sørensen, K. Zahlsen, A. Hyldbakk, E. F. da Silva and A. M. Booth, Photodegradation in natural waters of nitrosamines and nitramines derived from CO<sub>2</sub> capture plant operation, *Int. J. Greenhouse Gas Control*, 2015, **32**, 106–114, DOI: [10.1016/j.ijggc.2014.11.004](https://doi.org/10.1016/j.ijggc.2014.11.004).
- 13 A. Afzal, J. Kang, B. M. Choi and H. J. Lim, Degradation and fate of N-nitrosamines in water by UV photolysis, *Int. J. Greenhouse Gas Control*, 2016, **52**, 44–51, DOI: [10.1016/j.ijggc.2016.06.009](https://doi.org/10.1016/j.ijggc.2016.06.009).
- 14 N. Dai and W. A. Mitch, Influence of Amine Structural Characteristics on N-Nitrosamine Formation Potential Relevant to Postcombustion CO<sub>2</sub> Capture Systems, *Environ. Sci. Technol.*, 2013, **47**(22), 13175–13183, DOI: [10.1021/es4035396](https://doi.org/10.1021/es4035396).
- 15 Z. Wang and W. A. Mitch, Influence of Dissolved Metals on N-Nitrosamine Formation under Amine-based CO<sub>2</sub> Capture Conditions, *Environ. Sci. Technol.*, 2015, **49**(19), 11974–11981, DOI: [10.1021/acs.est.5b03085](https://doi.org/10.1021/acs.est.5b03085).
- 16 S. Lindahl, C. Brecke Gundersen and E. Lundanes, A review of available analytical technologies for qualitative and quantitative determination of nitramines, *Environ. Sci.: Processes Impacts*, 2014, **16**(8), 1825–1840, DOI: [10.1039/C4EM00095A](https://doi.org/10.1039/C4EM00095A).
- 17 M. Låg, B. Lindeman, C. Instanes, G. Brunborg and P. E. Schwarze, Health effects of amines and derivatives associated with CO<sub>2</sub> capture. 44. Nasjonalt folkehelseinstitutt; 2011. Available from: <https://fhi.brage.unit.no/fhi-xmlui/handle/11250/2688582>.
- 18 C. Svendsen, M. Låg, M. Andreassen, B. Granum and B. Lindeman, New knowledge on health effects of amines and their derivatives associated with CO<sub>2</sub> capture. Folkehelseinstituttet, 2024. Available from: <https://fhi.brage.unit.no/fhi-xmlui/handle/11250/3153037>.
- 19 EMA, Nitrosamines EMEA-H-A5(3)-1490 - Assessment report, Amsterdam, European Medicines Agency (EMA), The Netherlands, 2020, p. 98. Report No.: EMA/369136/2020. Available from: [https://www.ema.europa.eu/en/documents/opinion-any-scientific-matter/nitrosamines-emea-h-a53-1490-assessment-report\\_en.pdf](https://www.ema.europa.eu/en/documents/opinion-any-scientific-matter/nitrosamines-emea-h-a53-1490-assessment-report_en.pdf).
- 20 M. van B. Z. en Koninkrijksrelaties, Drinkwaterbesluit [AMvB], Netherlands, 2024. Report No.: BWBR0030111. Available from: <https://wetten.overheid.nl/BWBR0030111/2024-01-01/0/informatie>.
- 21 X. Li, E. Bei, Y. Qiu, H. Xiao, J. Wang and P. Lin, *et al.*, Intake of volatile nitrosamines by Chinese residents in different provinces via food and drinking water, *Sci. Total Environ.*, 2021, **754**, 142121, DOI: [10.1016/j.scitotenv.2020.142121](https://doi.org/10.1016/j.scitotenv.2020.142121).
- 22 A. E. Poste, M. Grung and R. F. Wright, Amines and amine-related compounds in surface waters: A review of sources, concentrations and aquatic toxicity, *Sci. Total Environ.*, 2014, **481**, 274–279, DOI: [10.1016/j.scitotenv.2014.02.066](https://doi.org/10.1016/j.scitotenv.2014.02.066).
- 23 X. Ge, A. S. Wexler and S. L. Clegg, Atmospheric amines – Part I. A review, *Atmos. Environ.*, 2011, **45**(3), 524–546, DOI: [10.1016/j.atmosenv.2010.10.012](https://doi.org/10.1016/j.atmosenv.2010.10.012).
- 24 N. J. Farren, N. Ramírez, J. D. Lee, E. Finessi, A. C. Lewis and J. F. Hamilton, Estimated Exposure Risks from Carcinogenic Nitrosamines in Urban Airborne Particulate Matter, *Environ. Sci. Technol.*, 2015, **49**(16), 9648–9656, DOI: [10.1021/acs.est.5b01620](https://doi.org/10.1021/acs.est.5b01620).
- 25 T. T. H. Mai and H. Kim, Occurrence of N-nitrosamines in the atmosphere and human health risk: A case study in an urban area of Chuncheon, Gangwon State, South Korea, *Environ. Pollut.*, 2024, **349**, 123802, DOI: [10.1016/j.envpol.2024.123802](https://doi.org/10.1016/j.envpol.2024.123802).
- 26 N. R. Choi, Y. G. Ahn, J. Y. Lee, E. Kim, S. Kim and S. M. Park, *et al.*, Particulate Nitrosamines and Nitramines in Seoul and Their Major Sources: Primary Emission versus Secondary Formation, *Environ. Sci. Technol.*, 2021, **55**(12), 7841–7849, DOI: [10.1021/acs.est.1c01503](https://doi.org/10.1021/acs.est.1c01503).
- 27 J. Xia, Y. Chen, H. Huang, H. Li, D. Huang and Y. Liang, *et al.*, Occurrence and mass loads of N-nitrosamines discharged from different anthropogenic activities in Desheng River, South China, *Environ. Sci. Pollut. Res.*, 2023, **30**(20), 57975–57988, DOI: [10.1007/s11356-023-26458-8](https://doi.org/10.1007/s11356-023-26458-8).
- 28 J. W. A. Charrois, J. M. Boyd, K. L. Froese and S. E. Hrudey, Occurrence of N-nitrosamines in Alberta public drinking-water distribution systems, *J. Environ. Eng. Sci.*, 2007, **6**(1), 103–114, DOI: [10.1139/s06-031](https://doi.org/10.1139/s06-031).
- 29 S. S. Walse and W. A. Mitch, Nitrosamine Carcinogens Also Swim in Chlorinated Pools, *Environ. Sci. Technol.*, 2008, **42**(4), 1032–1037, DOI: [10.1021/es702301p](https://doi.org/10.1021/es702301p).
- 30 EEA, Europe's groundwater: a key resource under pressure, European Environment Agency (EEA), Publications Office of the European Union, 2022. Available from: <https://data.europa.eu/doi/10.2800/50592>.
- 31 EurEau, Europe's Water in Figures: An overview of the European drinking water and waste water sectors. 2021. 37 p. Available from: <https://www.eureau.org/resources/publications/eureau-publications/5824-europe-s-water-in-figures-2021/file>.
- 32 M. Karl, R. F. Wright, T. F. Berglen and B. Denby, Worst case scenario study to assess the environmental impact of amine emissions from a CO<sub>2</sub> capture plant, *Int. J. Greenhouse Gas Control*, 2011, **5**(3), 439–447, DOI: [10.1016/j.ijggc.2010.11.001](https://doi.org/10.1016/j.ijggc.2010.11.001)The 5th Trondheim Conference on CO<sub>2</sub> Capture, Transport and Storage.
- 33 M. Karl, N. Castell, D. Simpson, S. Solberg, J. Starrfelt and T. Svendby, *et al.*, Uncertainties in assessing the environmental impact of amine emissions from a CO<sub>2</sub> capture plant. Atmospheric, *Chem. Phys.*, 2014, **14**(16), 8533–8557, DOI: [10.5194/acp-14-8533-2014](https://doi.org/10.5194/acp-14-8533-2014).
- 34 Frederik Neuwahl, Gianluca Cusano, Jorge Gómez Benavides, Simon Holbrook and Serge Roudier. Best Available Techniques (BAT) reference document for waste incineration: Industrial Emissions Directive 2010/75/EU (Integrated Pollution Prevention and Control) [Internet]. Publications Office of the European Union; 2019 [cited 2026 Mar 26]. Report No. Available from: <https://data.europa.eu/doi/10.2760/761437>.
- 35 P. Javadi, P. O'Rourke, J. Fuhrman, H. McJeon, S. C. Doney and W. Shobe, *et al.*, The impact of regional resources and



- technology availability on carbon dioxide removal potential in the United States, *Environ. Res.: Energy*, 2024, **1**(4), 045007, DOI: [10.1088/2753-3751/ad81fb](https://doi.org/10.1088/2753-3751/ad81fb).
- 36 A. R. J. van der, J. Ding and H. Eskes, Monitoring European anthropogenic NO<sub>x</sub> emissions from space. Atmospheric, *Chem. Phys.*, 2024, **24**(13), 7523–7534, DOI: [10.5194/acp-24-7523-2024](https://doi.org/10.5194/acp-24-7523-2024).
- 37 EU Directive 2000/60/EC. OJ L. 2000 Oct 23. Available from: <https://data.europa.eu/eli/dir/2000/60/oj/eng>.
- 38 P. Raskin, P. Gleick, P. Kirshen, G. Pontius and K. Strzepek, Comprehensive assessment of the freshwater resources of the world:: report of the Secretary-General. UN,; 1997 Feb [cited 2025 Apr 24]. Report No. Available from: <https://digitallibrary.un.org/record/231336>.
- 39 M. N. Sondermann and R. Proença de Oliveira, Using the WEI+ index to evaluate water scarcity at highly regulated river basins with conjunctive uses of surface and groundwater resources, *Sci. Total Environ.*, 2022, **836**, 155754, DOI: [10.1016/j.scitotenv.2022.155754](https://doi.org/10.1016/j.scitotenv.2022.155754).
- 40 EEA, ArcGIS Rest API, 2025, Available from: <https://bio.discomap.eea.europa.eu/arcgis/rest/services>.
- 41 A. R. J. van der, J. Ding and H. Eskes, Monitoring European anthropogenic NO<sub>x</sub> emissions from space. Atmospheric, *Chem. Phys.*, 2024, **24**(13), 7523–7534, DOI: [10.5194/acp-24-7523-2024](https://doi.org/10.5194/acp-24-7523-2024).
- 42 J. P. Veefkind, I. Aben, K. McMullan, H. Förster, J. de Vries and G. Otter, *et al.*, TROPOMI on the ESA Sentinel-5 Precursor: A GMES mission for global observations of the atmospheric composition for climate, air quality and ozone layer applications, *Remote Sens Environ.*, 2012, **120**, 70–83, DOI: [10.1016/j.rse.2011.09.027](https://doi.org/10.1016/j.rse.2011.09.027)The Sentinel Missions - New Opportunities for Science.
- 43 Z. Zajac, O. Gomez, E. Gelati, M. van der Velde, S. Bassu and A. Ceglar, *et al.*, Estimation of spatial distribution of irrigated crop areas in Europe for large-scale modelling applications, *Agric. Water Manage.*, 2022, **266**, 107527, DOI: [10.1016/j.agwat.2022.107527](https://doi.org/10.1016/j.agwat.2022.107527).
- 44 WorldPop., Individual Countries 1km UN Adjusted Population Density (2000–2020) [Internet]. University of Southampton; 2025 [cited 2026 Mar 26], DOI: [10.5258/SOTON/WP00675](https://doi.org/10.5258/SOTON/WP00675). Available from: <https://www.worldpop.org/doi/10.5258/SOTON/WP00675>.
- 45 H. Hersbach, B. Bell, P. Berrisford, G. Biavati, A. Horányi, J. Muñoz Sabater, J. Nicolas, C. Peubey, R. Radu, I. Rozum, D. Schepers, A. Simmons, C. Soci, D. Dee and J.-N. Thépaut ERA5 hourly data on single levels from 1940 to present. Copernicus Climate Change Service (C3S) Climate Data Store (CDS), 2023. Available from: DOI: [10.24381/cds.adbb2d47](https://doi.org/10.24381/cds.adbb2d47).
- 46 C. B. Gundersen, M. D. Norling and A. S. Gagne, Modelling future levels of nitrosamines and nitramines in a groundwater compartment close to a CO<sub>2</sub> capture facility, 27, Norsk institutt for vannforskning, 2024. Available from: <https://niva.brage.unit.no/niva-xmlui/handle/11250/3160694>.
- 47 B. Languille, A. Drageset, T. Mikoviny, E. Zardin, C. Benquet, Ø. Ullestad, *et al.*, Atmospheric Emissions of Amino-Methyl-Propanol, Piperazine and Their Degradation Products During the 2019–20 ALIGN-CCUS Campaign at the Technology Centre Mongstad [SSRN Scholarly Paper] [Internet]. Rochester, NY: Social Science Research Network; 2021 [cited 2026 Mar 26], DOI: [10.2139/ssrn.3812139](https://doi.org/10.2139/ssrn.3812139). Available from: <https://papers.ssrn.com/abstract=3812139>.
- 48 J. Mertens, J. Knudsen, M. L. Thielens and J. Andersen, On-line monitoring and controlling emissions in amine post combustion carbon capture: A field test, *Int. J. Greenhouse Gas Control*, 2012, **6**, 2–11, DOI: [10.1016/j.ijggc.2011.11.015](https://doi.org/10.1016/j.ijggc.2011.11.015).
- 49 J. Gibbins and M. Lucquiaud BAT Review for New-Build and Retrofit Post-Combustion Carbon Dioxide Capture Using Amine-Based Technologies for Power and CHP Plants Fuelled by Gas and Biomass and for Post-Combustion Capture Using Amine-Based and Hot Potassium Carbonate Technologies on EfW Plants as Emerging Technologies under the IED for the UK. Ver.2.0 [Internet]. University of Sheffield; 2022 [cited 2025 Nov 12]. Report No. Available from: <https://ukccsrc.ac.uk/best-available-technologybat-information-for-ccs/>.
- 50 V. Buvik, A. Grimstvedt, K. Vernstad, H. K. Knuutila, M. Zeeshan and S. Akhter, *et al.*, CESAR1 solvent degradation in pilot and laboratory scale, *Int. J. Greenhouse Gas Control*, 2026, **150**, 104560, DOI: [10.1016/j.ijggc.2025.104560](https://doi.org/10.1016/j.ijggc.2025.104560).
- 51 E. F. da Silva, K. A. Hoff and A. Booth, Emissions from CO<sub>2</sub> capture plants; an overview, *Energy Procedia*, GHGT-11 Proceedings of the 11th International Conference on Greenhouse Gas Control Technologies, 18-22 November 2012, Kyoto, Japan, 2013;37:784–790, DOI: [10.1016/j.egypro.2013.05.168](https://doi.org/10.1016/j.egypro.2013.05.168).
- 52 P. Khakharia, H. M. Kvamsdal, E. F. da Silva, T. J. H. Vlugt and E. Goetheer, Field study of a Brownian Demister Unit to reduce aerosol based emission from a Post Combustion CO<sub>2</sub> Capture plant, *Int. J. Greenhouse Gas Control*, 2014, **28**, 57–64, DOI: [10.1016/j.ijggc.2014.06.022](https://doi.org/10.1016/j.ijggc.2014.06.022).
- 53 L. Liu, X. Wang, H. Wang, T. Wang and M. Fang, Aerosol emissions and mitigation of aqueous AMP/PZ solvent for postcombustion CO<sub>2</sub> capture, *Carbon Capture Sci. Technol.*, 2024, **13**, 100273, DOI: [10.1016/j.cst.2024.100273](https://doi.org/10.1016/j.cst.2024.100273).
- 54 P. Chen, D. Wang, N. Yi, J. Jiang, L. Herraiz and X. Zhou, *et al.*, Amine-based carbon capture through an environmental lens: Amine emissions and associated implications, *J. Environ. Chem. Eng.*, 2025, **13**(6), 119605, DOI: [10.1016/j.jece.2025.119605](https://doi.org/10.1016/j.jece.2025.119605).
- 55 D. Tønnesen, CO<sub>2</sub>-rensing Klemetsrud. Beregning av nitrosog nitraminer. [Internet]. Oslo, Norway: NILU; [cited 2026 Feb 25]. p. 13. Report No.: NILU rapport 11/2018. Available from: <https://hdl.handle.net/11250/3049082>.
- 56 E. Custodio, Coastal aquifers of Europe: an overview, *Hydrogeol. J.*, 2010, **18**(1), 269–280, DOI: [10.1007/s10040-009-0496-1](https://doi.org/10.1007/s10040-009-0496-1).
- 57 M. Kramer and P. N. M. Schipper, Waterwingebied Sint-Jansteen: Modelling punt- en diffuse bronnen en optimalisatie waterwinning. Grontmij, Netherlands, 2010, p. 48. Report No.: 13/99099520/MK. Available from: [https://zeeland.nazca4u.nl/documenten/locaties/99727\\_Modellering%20grondwater%20St.%20Jansteen%2023%20juli%202010.pdf](https://zeeland.nazca4u.nl/documenten/locaties/99727_Modellering%20grondwater%20St.%20Jansteen%2023%20juli%202010.pdf).



- 58 C. van den Brink, G. Frapporti, J. Griffioen and W. J. Zaadnoordijk, Statistical analysis of anthropogenic versus geochemical-controlled differences in groundwater composition in The Netherlands, *J. Hydrol.*, 2007, **336**(3), 470–480, DOI: [10.1016/j.jhydrol.2007.01.024](https://doi.org/10.1016/j.jhydrol.2007.01.024).
- 59 A. Visser, H. P. Broers, R. Heerdink and M. F. P. Bierkens, Trends in pollutant concentrations in relation to time of recharge and reactive transport at the groundwater body scale, *J. Hydrol.*, 2009, **369**(3), 427–439, DOI: [10.1016/j.jhydrol.2009.02.008](https://doi.org/10.1016/j.jhydrol.2009.02.008).
- 60 G. J. Houben, V. E. A. Post, J. Gröger-Trampe, M. H. Pesci and J. Sültenfuß, On the Propagation of Reaction Fronts in a Sandy Aquifer Over 20+ Years: Lessons From a Test Site in Northwestern Germany, *Water Resour. Res.*, 2021, **57**(8), e2020WR028706, DOI: [10.1029/2020WR028706](https://doi.org/10.1029/2020WR028706).
- 61 T. Röper, K. F. Kröger, H. Meyer, J. Sültenfuß, J. Greskowiak and G. Massmann, Groundwater ages, recharge conditions and hydrochemical evolution of a barrier island freshwater lens (Spiekeroog, Northern Germany), *J. Hydrol.*, 2012, **454–455**, 173–186, DOI: [10.1016/j.jhydrol.2012.06.011](https://doi.org/10.1016/j.jhydrol.2012.06.011).
- 62 S. Mattern, D. Fasbender and M. Vanclooster, Discriminating sources of nitrate pollution in an unconfined sandy aquifer, *J. Hydrol.*, 2009, **376**(1), 275–284, DOI: [10.1016/j.jhydrol.2009.07.039](https://doi.org/10.1016/j.jhydrol.2009.07.039).
- 63 M. Vanclooster, D. Pinte and M. Javaux, Estimation des temps de transfert de nitrates dans le sous-sol de la zone vulnérable des sables du Bruxellien. [Technical Report]. Louvain, Belgium: Université catholique de Louvain; 2004. Report No.
- 64 J. E. Vermaat, S. Broekx, B. Van Eck, G. Engelen, F. Hellmann, J. De Kok, H. Van der Kwast, J. Maes, W. Salomons and W. Van Deursen, Nitrogen Source Apportionment for the Catchment, Estuary, and Adjacent Coastal Waters of the River Scheldt, *Ecol. Soc.*, 2012, **17**(2), 30, DOI: [10.5751/ES-04889-170230](https://doi.org/10.5751/ES-04889-170230).
- 65 GRDC. The Global Runoff Data Centre, 56068 Koblenz, Germany, 2025. The Global Runoff Data Centre, 56068 Koblenz, Germany. Available from: <https://grdc.bafg.de/>.
- 66 A. Bannink, M. Van der Ploeg, T. Oomen and A. Wagenvoort, Jaarrapport 2020 De Maas, Association of River Waterworks, RIWA, Maastricht, The Netherlands, 2021. Available from: <https://www.riwa-maas.org/wp-content/uploads/2021/09/IDF2627-RIWA-MAAS-Jaarrapport-NL-2020-digitaal-1.pdf>.
- 67 L. Sonesten, P. Axe, B. Bellert, L. Burtschell, D. Eumont, V. Fairbank, *et al.*, Waterborne and Atmospheric Inputs of Nutrients and Metals to the Sea, OSPAR, 2023: The 2023 Quality Status Report for the Northeast Atlantic. OSPAR Commission, London., 2022. Available from: <https://oap.ospar.org/en/ospar-assessments/quality-status-reports/qsr-2023/other-assessments/inputs-nutrients-and-metals>.
- 68 M. D. Norling Mobius2 [Internet]. Oslo, Norway: NIVA; 2025 [cited 2026 Mar 26]. Available from: <https://nivanorge.github.io/Mobius2/>.
- 69 L. Nizzetto, D. Butterfield, M. Futter, Y. Lin, I. Allan and T. Larssen, Assessment of contaminant fate in catchments using a novel integrated hydrobiogeochemical-multimedia fate model, *Sci. Total Environ.*, 2016, **544**, 553–563, DOI: [10.1016/j.scitotenv.2015.11.087](https://doi.org/10.1016/j.scitotenv.2015.11.087).
- 70 B. Lehner and G. Grill, Global river hydrography and network routing: baseline data and new approaches to study the world's large river systems, *Hydrol. Processes*, 2013, **27**(15), 2171–2186, DOI: [10.1002/hyp.9740](https://doi.org/10.1002/hyp.9740).
- 71 P. Zippenfenig, Open-Meteo.com Weather API, Zenodo; 2024, DOI: [10.5281/zenodo.14582479](https://doi.org/10.5281/zenodo.14582479). Available from: <https://zenodo.org/records/14582479>.
- 72 D. Pichot, L. Granados, T. Morel, A. Schuller, R. Dubettier and F. Lockwood, Start-up of Port-Jérôme CRYOCAPT M Plant: Optimized Cryogenic CO<sub>2</sub> Capture from H<sub>2</sub> Plants, *Energy Procedia*, 2017, **114**, 2682–2689, DOI: [10.1016/j.egypro.2017.03.1532](https://doi.org/10.1016/j.egypro.2017.03.1532).
- 73 K. Atsonios, K. Panopoulos, P. Grammelis and E. Kakaras, Exergetic comparison of CO<sub>2</sub> capture techniques from solid fossil fuel power plants, *Int. J. Greenhouse Gas Control*, 2016, **45**, 106–117, DOI: [10.1016/j.ijggc.2015.12.022](https://doi.org/10.1016/j.ijggc.2015.12.022).
- 74 Z. Zhang, Continuous Recycling CO<sub>2</sub> Capture System With Alkali Based Absorbent and Simulation, *Proc CSEE*, 2022, **42**(16), 5989–5995, DOI: [10.13334/j.0258-8013.pcsee.211438](https://doi.org/10.13334/j.0258-8013.pcsee.211438).
- 75 A. M. James, J. Reynolds, D. G. Reed, P. Styring and R. Dawson, A Pressure Swing Approach to Selective CO<sub>2</sub> Sequestration Using Functionalized Hypercrosslinked Polymers, *Materials*, 2021, **14**(7), 7, DOI: [10.3390/ma14071605](https://doi.org/10.3390/ma14071605).
- 76 R. Cooper, D. Bove, E. Audasso, M. C. Ferrari and B. Bosio, A feasibility assessment of a retrofit Molten Carbonate Fuel Cell coal-fired plant for flue gas CO<sub>2</sub> segregation, *Int. J. Hydrogen Energy*, 2021, **46**(28), 15024–15031, DOI: [10.1016/j.ijhydene.2020.09.189](https://doi.org/10.1016/j.ijhydene.2020.09.189).
- 77 Spherical Insights, Europe Amines Market Size, Share, and COVID-19 Impact Analysis, By Product (Ethanolamine, Fatty Amines, Alkyl Amines, and Others), By Application (Crop Protection, Surfactants, Water Treatment, Personal Care, Gas Treatment, and Others), and Europe Amines Market Insights, Industry Trend, Forecasts to 2033, 2024, p. 210. Report No.: SI7322. Available from: <https://www.sphericalinsights.com/reports/europe-amines-market>.
- 78 P. H. M. Feron, A. Cousins, K. Jiang, R. Zhai and M. Garcia, An update of the benchmark post-combustion CO<sub>2</sub>-capture technology, *Fuel*, 2020, **273**, 117776, DOI: [10.1016/j.fuel.2020.117776](https://doi.org/10.1016/j.fuel.2020.117776).
- 79 S. Zhang, Y. Shen, C. Zheng, Q. Xu, Y. Sun and M. Huang, *et al.*, Recent advances, challenges, and perspectives on carbon capture, *Front. Environ. Sci. Eng.*, 2024, **18**(6), 75, DOI: [10.1007/s11783-024-1835-0](https://doi.org/10.1007/s11783-024-1835-0).
- 80 L. B. Hamdy, A. Goel C, R. Rudd J, A. Barron and E. Andreoli, The application of amine-based materials for carbon capture and utilisation: an overarching view, *Mater. Adv.*, 2021, **2**(18), 5843–5880, DOI: [10.1039/D1MA00360G](https://doi.org/10.1039/D1MA00360G).
- 81 T. M. Thiedemann and M. Wark, A Compact Review of Current Technologies for Carbon Capture as Well as Storing and Utilizing the Captured CO<sub>2</sub>, *Processes*, 2025, **13**(1), 1, DOI: [10.3390/pr13010283](https://doi.org/10.3390/pr13010283).



- 82 X. Miklin, T. Neier, S. Sturn and K. Zwickl, Carbon Giants: Exploring the Top 100 Industrial CO<sub>2</sub> Emitters in the EU, *Ecol. Econ.*, 2025, **228**, 108419, DOI: [10.1016/j.ecolecon.2024.108419](https://doi.org/10.1016/j.ecolecon.2024.108419).
- 83 O. G. Brakstad, L. Sørensen, K. Zahlse, K. Bonaunet, A. Hyldbakk and A. M. Booth, Biotransformation in water and soil of nitrosamines and nitramines potentially generated from amine-based CO<sub>2</sub> capture technology, *Int. J. Greenhouse Gas Control*, 2018, **70**, 157–163, DOI: [10.1016/j.ijggc.2018.01.021](https://doi.org/10.1016/j.ijggc.2018.01.021).
- 84 X. Chen, G. Huang, C. An, Y. Yao and S. Zhao, Emerging N-nitrosamines and N-nitramines from amine-based post-combustion CO<sub>2</sub> capture – A review, *Chem. Eng. J.*, 2018, **335**, 921–935, DOI: [10.1016/j.cej.2017.11.032](https://doi.org/10.1016/j.cej.2017.11.032).
- 85 D. N. Moriasi, M. W. Gitau, N. Pai and P. Daggupati, Hydrologic and Water Quality Models: Performance Measures and Evaluation Criteria, *Trans. ASABE.*, 2015, **58**(6), 1763–1785, DOI: [10.13031/trans.58.10715](https://doi.org/10.13031/trans.58.10715).
- 86 C. Brecke Gundersen, A. Wisthaler, M. Cassiani, M. D. Norling, A. C. Wennberg, F. Clayer, *et al.*, A Dynamic Modelling Tool to Ensure the Safety of Drinking Water Sources Near Amine-Based CO<sub>2</sub> Capture Plants [SSRN Scholarly Paper], Social Science Research Network, Rochester, NY, 2024. Available from: <https://papers.ssrn.com/abstract=5020993>, DOI: [10.2139/ssrn.5020993](https://doi.org/10.2139/ssrn.5020993).
- 87 WHO, Chemical fact sheets: N-nitrosodimethylamine (NDMA), 2022. Report No. Available from: <https://www.who.int/publications/m/item/chemical-fact-sheets-n-nitrosodimethylamine-ndma>.
- 88 G. T. Rochelle, Air pollution impacts of amine scrubbing for CO<sub>2</sub> capture, *Carbon Capture Sci. Technol.*, 2024, **11**, 100192, DOI: [10.1016/j.ccst.2024.100192](https://doi.org/10.1016/j.ccst.2024.100192).
- 89 N. Borduas, J. P. D. Abbatt and J. G. Murphy, Gas Phase Oxidation of Monoethanolamine (MEA) with OH Radical and Ozone: Kinetics, Products, and Particles, *Environ. Sci. Technol.*, 2013, **47**(12), 6377–6383, DOI: [10.1021/es401282j](https://doi.org/10.1021/es401282j).
- 90 C. J. Nielsen, B. D'Anna, C. Dye, C. George, M. Graus, A. Hansel, *et al.*, Atmospheric Degradation of Amines (ADA) Summary Report: Gas phase photo-oxidation of 2-aminoethanol (MEA) [Internet]. Oslo, Norway: NILU; 2010 [cited 2026 Feb 25]. p. 70. Report No.: NILU OR 8/2010. Available from: [https://nilu.no/wp-content/uploads/dnn/08-2010-CJN\\_MKA\\_ADA-report1.pdf](https://nilu.no/wp-content/uploads/dnn/08-2010-CJN_MKA_ADA-report1.pdf).
- 91 W. Tan, L. Zhu, T. Mikoviny, C. J. Nielsen, A. Wisthaler and B. D'Anna, *et al.*, Experimental and Theoretical Study of the OH-Initiated Degradation of Piperazine under Simulated Atmospheric Conditions, *J. Phys. Chem. A.*, 2021, **125**(1), 411–422, DOI: [10.1021/acs.jpca.0c10223](https://doi.org/10.1021/acs.jpca.0c10223).
- 92 C. J. Nielsen, B. D'Anna, M. Aursnes, A. Boreave, R. Rossi, A. J. C. Bunkan, *et al.*, Atmospheric Degradation of Amines (ADA). Summary report: Photo-oxidation of methylamine, dimethylamine and trimethylamine. [Internet]. Oslo, Norway: NILU; 2011 [cited 2026 Feb 25]. Report No.: NILU OR 02/2011. Available from: <https://nilu.no/publikasjon/25495/>.
- 93 W. Tan, L. Zhu, T. Mikoviny, C. J. Nielsen, Y. Tang and A. Wisthaler, *et al.*, Atmospheric Chemistry of 2-Amino-2-methyl-1-propanol: A Theoretical and Experimental Study of the OH-Initiated Degradation under Simulated Atmospheric Conditions, *J. Phys. Chem. A.*, 2021, **125**(34), 7502–7519, DOI: [10.1021/acs.jpca.1c04898](https://doi.org/10.1021/acs.jpca.1c04898).
- 94 T. G. Almeida and T. Kurtén, Atmospheric Oxidation of Imine Derivative of Piperazine Initiated by OH Radical, *ACS Earth Space Chem.*, 2022, **6**(10), 2453–2464, DOI: [10.1021/acsearthspacechem.2c00170](https://doi.org/10.1021/acsearthspacechem.2c00170).

